No. 62-8

METALS IN KAMCHATKA MANTLE WEDGE LINKED TO CU-AU-AG DEPOSITS IN MAGMATIC ARCS

Kepezhinskas P.[1], Berdnikov N.[2], Kepezhinskas N.[3] , Konovalova N.[2]

1. pavel_k7@yahoo.com, Kosygin Institute of Tectonics and Geophysics, Khabarovsk, Russian Federation
2. Kosygin Institute of Tectonics and Geophysics, Khabarovsk, Russian Federation
3. kepezhin@ualberta.ca, Department of Earth and Atmospheric Science, University of Alberta, Edmonton, Canada

Geologic Setting and Xenolith Sites in Kamchatka

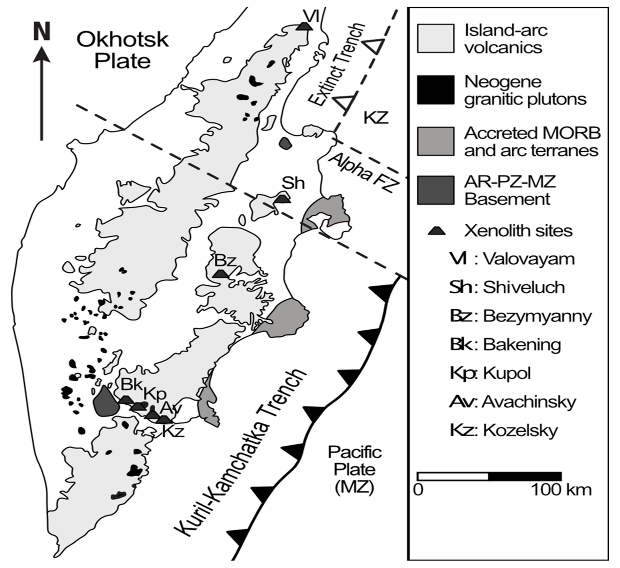

Figure 1. Tectonic setting and distribution of xenolith sites in Kamchatka. Avachinsky peridotite xenoliths are among the most depleted mantle samples in subduction zones. Presence of amphibole, bulk enrichments in some incompatible elements and Os-isotopes (Widom et al. 2003) suggest modal and cryptic metasomatism by subduction-related silicate melts and hydrous fluids.

Petrology of Peridotite Xenoliths

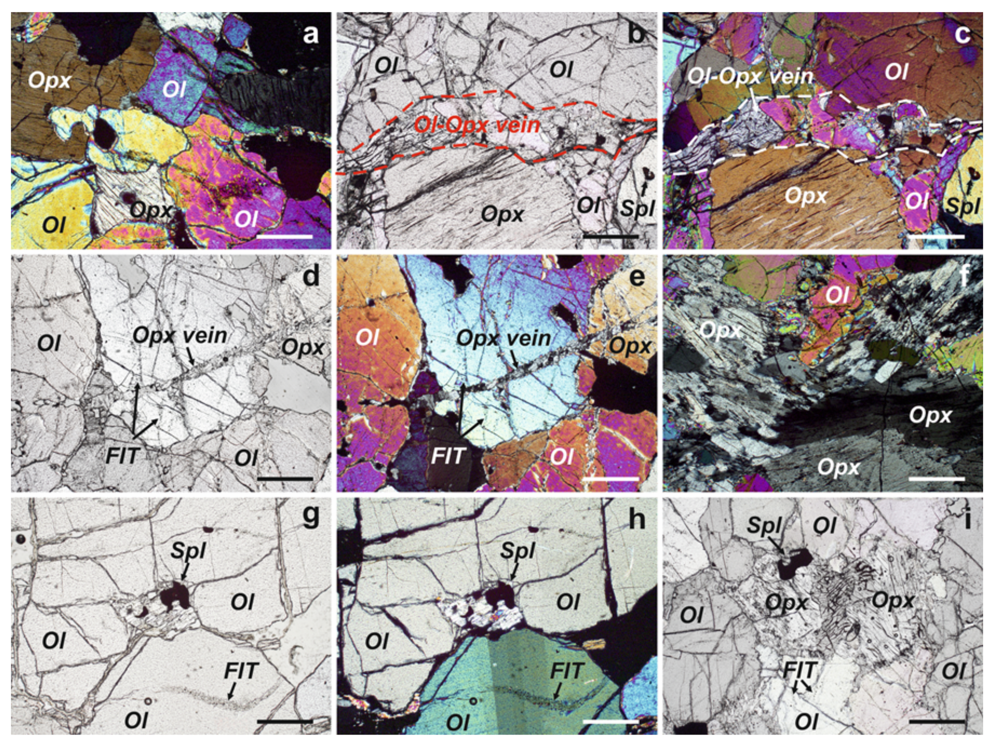

Figure 2. Petrography of Avachinsky peridotite xenoliths. (a) typical mosaic-porphyroclastic texture of Avachinsky spinel harzburgite (cross-polarized light); (b-c) olivine-orthopyroxene vein in spinel harzburgite (b – plane-polarized and c- cross-polarized light); (d-e) metasomatic orthopyroxene vein offsetting primary fluid inclusion trails (FIT) in harzburgite (d – plane-polarized and e – cross-polarized light); (f) mantle deformations (kink banding, blocky and undulose extinction, etc.) in orthopyroxene from spinel harzburgite (cross-polarized light); (g-h) fluid inclusion trails (FIT) in olivine (g – plane-polarized and h – cross-polarized light); (i) porphyroclastic texture of spinel harzburgite xenoliths with fluid inclusion trails (FIT) in large olivine porphyroclast (plane-polarized light). Ol – olivine, Opx- orthopyroxene, Spl – spinel. Scale bar in all images is 40 μm.

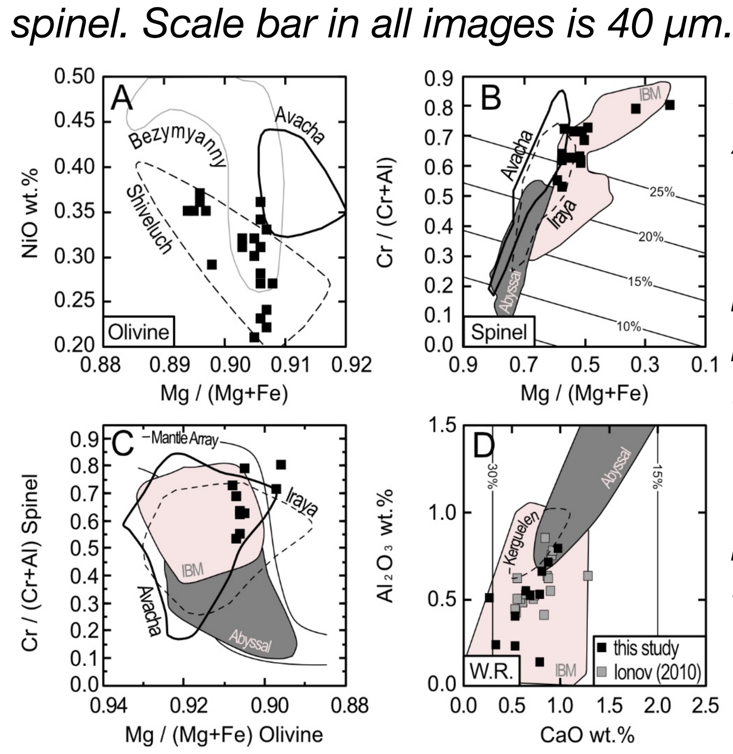

Figure 3. Mineral compositions in Avachinsky xenoliths (black squares). Fields for minerals from the Izu-Bonin-Mariana (IBM) fore-arc peridotites (Ishii et al., 1992), Iraya peridotite xenoliths (Yoshikawa et al., 2016), Avacha xenoliths (Ionov, 2010), Shiveluch and Bezymyanny xenoliths (Ionov et al., 2013) and abyssal peridotites (Dick and Bullen, 1984) are shown for comparison. (A) Mg/(Mg+Fe) vs. NiO in olivine. (B) Cr/(Cr+Al) vs. Mg/(Mg+Fe) in spinel. Partial melting degrees are from Hellebrand et al. (2001). (C) Mg/(Mg+Fe) in olivine vs. Cr/(Cr+Al) in spinel. Olivine-spinel mantle array is from Arai (1994). (D) Al2O3 vs. CaO in whole-rock peridotites (W.R.) Abyssal peridotite field is after Niu (2004). Kerguelen ultra-refractory peridotite xenoliths are from Wasilewski et al. (2017). Partial melting degrees are from Ishiwatari (1985).

Metals in Avachinsky Xenoliths

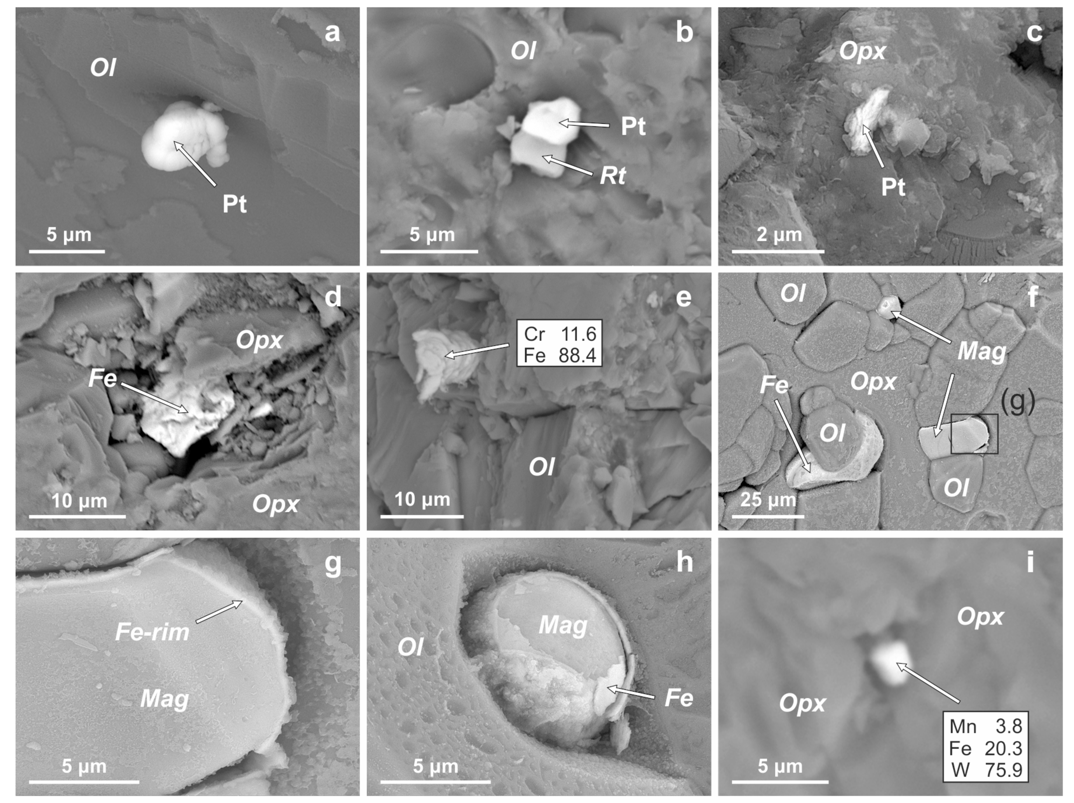

Figure 4. Siderophile metals in Avachinsky xenoliths. (a) Pt inclusion in olivine. (b) Equant Pt grain intergrown with rutile included in olivine. (c) Elongated euhedral platinum inclusion in orthopyroxene. (d) Native iron intergrown with orthopyroxene. (e) Cr-bearing Fe inclusion in olivine. (f) Textural relationships between euhedral magnetite, native Fe, olivine and orthopyroxene in harzburgite xenolith. Note magnetite covered by native iron intergrown with euhedral olivine grain. (g) Euhedral magnetite enveloped in native iron (Fe) rim. (h) Equant magnetite grain enveloped in native iron (Fe) film. (i) W-Fe-Mn inclusion in orthopyroxene. Ol – olivine, Opx – orthopyroxene, Mag – magnetite, Rt – rutile.

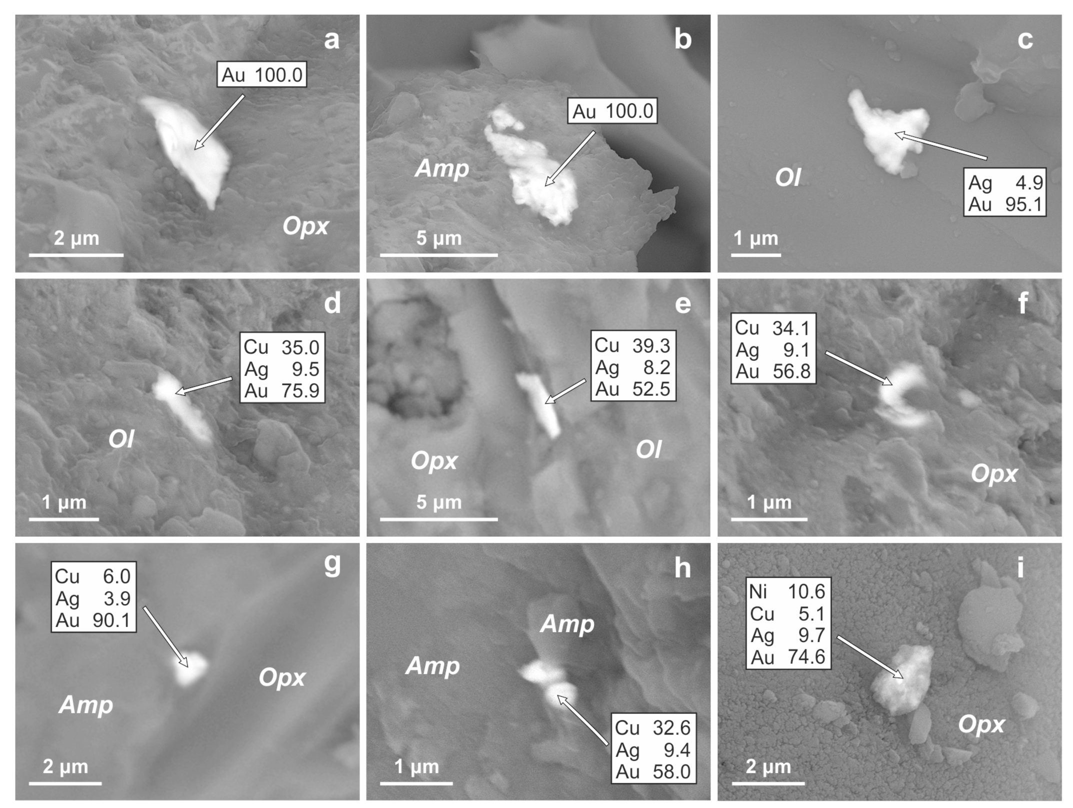

Figure 5. Gold and gold alloys in Avachinsky xenoliths. (a) Euhedral gold inclusion in orthopyroxene. (b) Partially disintegrated gold inclusion in amphibole. (c) Silver-bearing gold inclusion in olivine. (d) Elongated Cu-Au-Ag inclusion in olivine. (e) Elongated euhedral Cu-Au-Ag inclusion localized at a fracture-type boundary between olivine and orthopyroxene. (f) Curved (C-shaped) Cu-Au-Ag inclusion in orthopyroxene. (g) Equant Cu-Ag-bearing gold particle localized at the boundary between amphibole and orthopyroxene. (h) Cu-Au-Ag alloy intergrown with amphibole. (i) Nickel-copper-silver-gold inclusion on a broken surface of large orthopyroxene crystal. Ol – olivine, Opx – orthopyroxene, Ol – olivine.

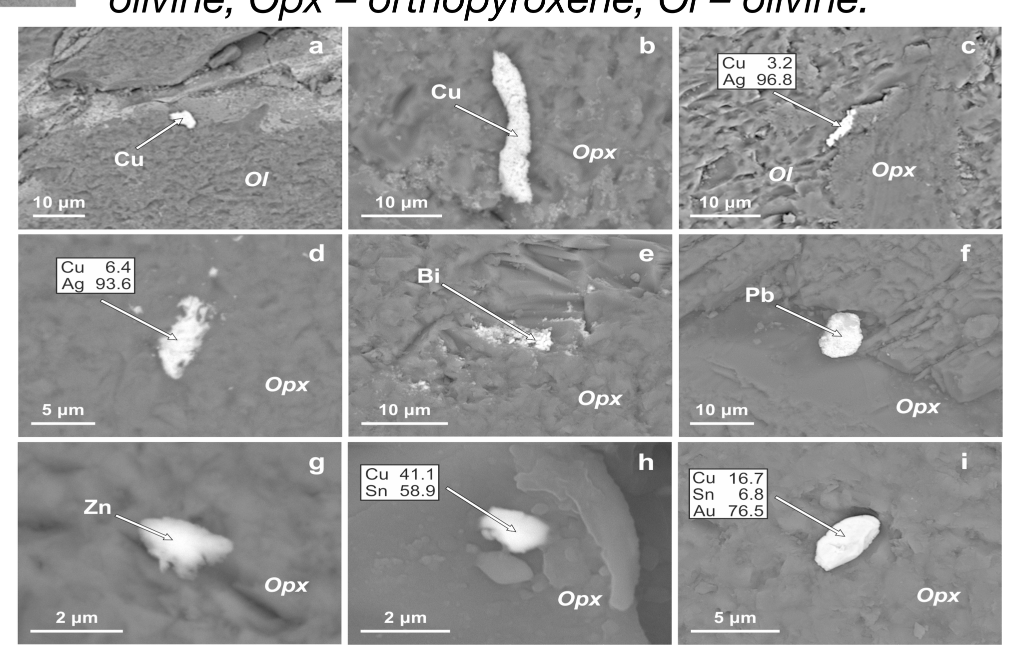

Figure 6. Chalcophile metals in Avachinsky xenoliths. (a) Equant copper inclusion in olivine. (b) Slightly bended, elongated copper inclusion in orthopyroxene. (c) Elongated Cu-bearing silver alloy located along the boundary between olivine and orthopyroxene. (d) Cu-bearing silver inclusion in orthopyroxene. (e) Partially disintegrated bismuth inclusion in orthopyroxene. (f) Equant lead inclusion in orthopyroxene. (g) Anhedral zinc inclusion in orthopyroxene. (h) Anhedral copper-tin inclusion in orthopyroxene. (i) Euhedral sculptured copper-tin-gold alloy included in orthopyroxene.

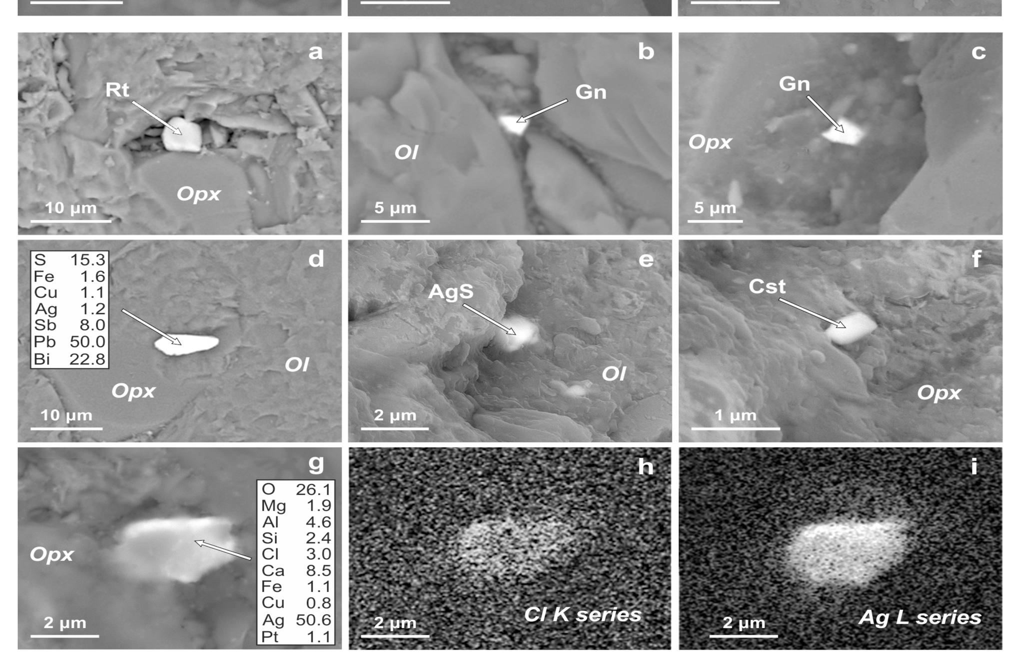

Figure 7. Minerals associated with metals in Avachinsky xenoliths. (a) Rutile inclusion in orthopyroxene. (b) Galena inclusion in olivine. (c) Galena inclusion in orthopyroxene. (d) Cu-Ag-bearing Sb-Bi-Pb sulfide phase localized at the contact between olivine and orthopyroxene. (e) Silver sulfide inclusion in olivine. (f) Cassiterite inclusion in orthopyroxene. (g-i) Chlorine-bearing silver inclusion in orthopyroxene: (g) backscatter electron image, (h) Cl K series map and (i) Ag L series map. Ol -olivine, Opx – orthopyroxene, Rt – rutile, Gn – galena, Cst – cassiterite.

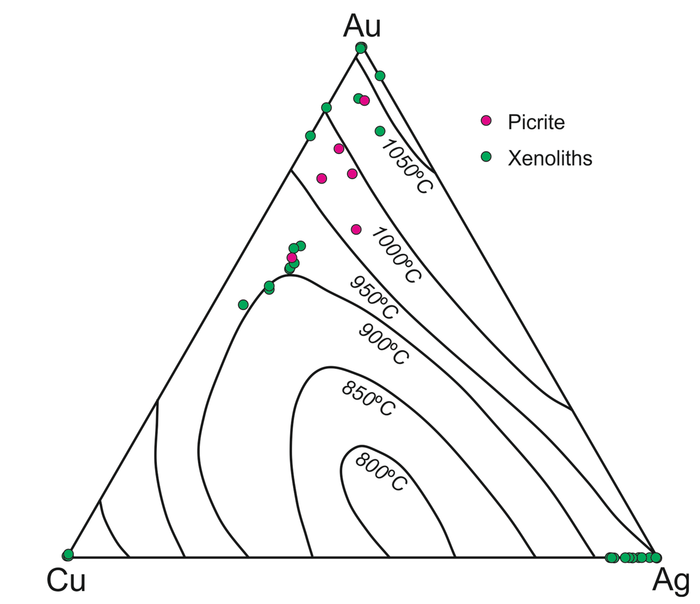

Figure 8. Composition of Cu-Ag-Au compounds from Avachinsky xenoliths and host picrite plotted on ternary phase diagram for Cu-Ag-Au system. Solid lines depict liquidus temperatures at different end-member compositions (Wise, 1964). Ubiquitous presence of Cu-Ag-Au alloys suggests that Cu and Au budgets of subduction-related porphyry and epithermal deposits can originate in metal-rich sub-arc mantle wedge.

Redox Conditions and Au-Pt Enrichments in the Kamchatka Mantle

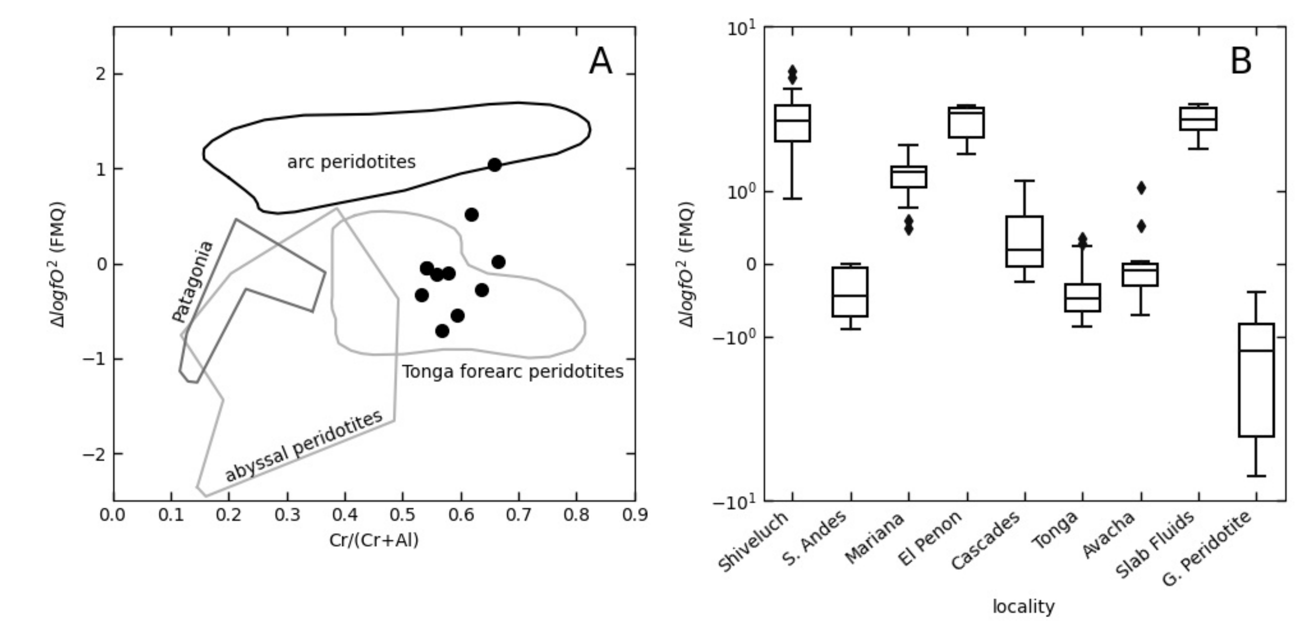

Figure 9. A. Variations of ΔlogfO2 (FMQ) versus Cr/(Cr+Al) in spinel for abyssal peridotites (Bryndzia and Wood, 1990), arc peridotites (Parkinson and Arculus, 1999), Tonga forearc peridotites (Birner et al., 2017), peridotite xenoliths from Patagonia (Wang et al., 2007) and Avacha xenoliths (black circles, Ionov, 2010). B. Variations of ΔlogfO2 (FMQ) in mantle wedge xenoliths from Shiveluch, Kamchatka (Bryant et al., 2007), Southern Andes (Wang et al., 2007), El Peñon, Mexico (Blatter and Carmichael, 1998), Avachinsky, Kamchatka (Ionov, 2010), Tonga forearc peridotites (Birner et al., 2017), basalts from the Marianas (Brounce et al., 2014) and the Cascades (Rowe et al., 2009), slab fluids (Iacovino et al., 2020) and mantle wedge garnet peridotites (Rielli et al., 2018). The data are plotted showing the range and maximum/minimum of analytical values (excluding outliers), the 25th and 75th percentiles and the median (excluding outliers).

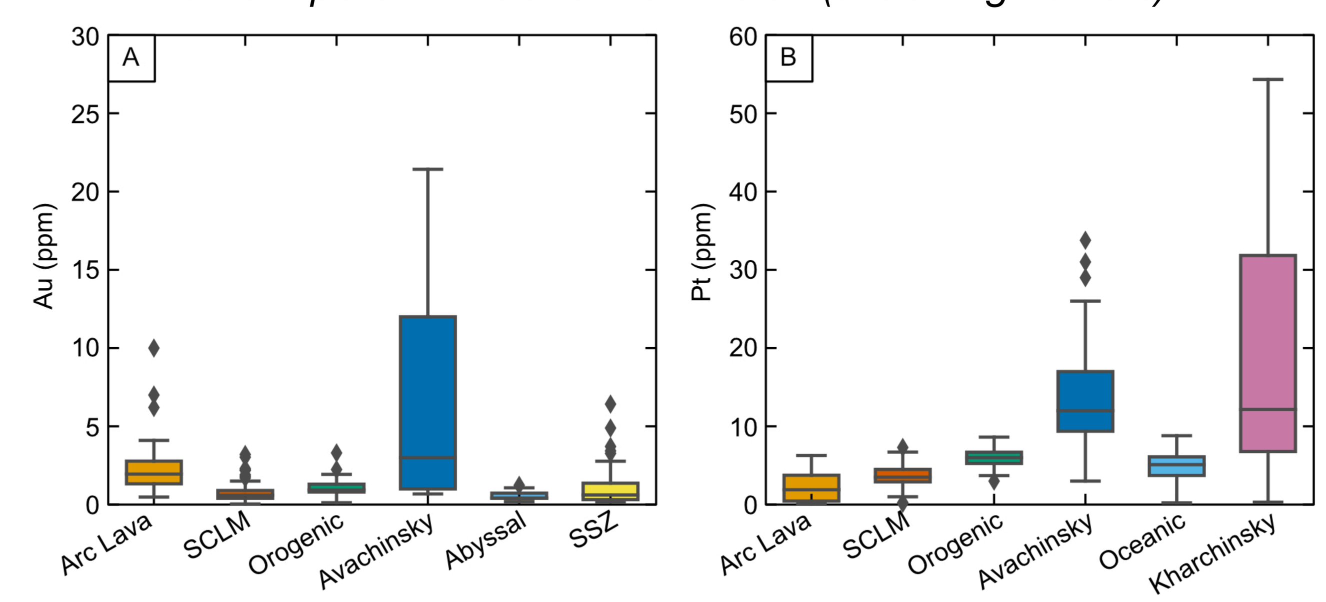

Figure 10. (Gold (A) and platinum (B) abundance in the Avachinsky harzburgite xenoliths compared to ultramafic xenoliths from the Kharchinsky volcano in central Kamchatka (Siegrist et al., 2021), abyssal peridotites (Snow and Schmidt, 1998; Luguet et al., 2003; Marchesi et al., 2013), orogenic lherzolites (Lorand et al., 1999; Fischer- Gödde et al., 2011; Saunders et al., 2018); supra-subduction zone (SSZ) ophiolitic peridotites (Oshin and Crocket, 1982; Saunders et al., 2018), subcontinental lithospheric mantle (SCLM; Mitchell and Keyas, 1981; Schmidt et al., 2003; Fischer- Gödde et al., 2011; Saunders et al., 2018), and arc lavas (Hamlyn et al., 1995; Woodland et al., 2002; Ivanov et al., 2008; Park et al., 2015). The data are plotted showing the range and maximum/minimum of analytical values (excluding outliers), the 25th and 75th percentiles and the median (excluding outliers).

Selected References

- Ionov D.A. (2010). Petrology of mantle wedge lithosphere: new data on supra-subduction peridotite xenoliths from the andesitic Avacha volcano, Kamchatka. Journal of Petrology, v. 51, p. 327-361.
- Widom, E., Kepezhinskas, P., Defant, M., 2003. The nature of metasomatism in the sub-arc mantle wedge: evidence from Re-Os isotopes in Kamchatka peridotite xenoliths. Chemical Geology 196, 283-306.
- Wise, J., 1964. Gold Recovery, Properties and Applications. D. Van Nostrand Company, Taylorville, Illinois, USA, 167p.